



ELSEVIER

Contents lists available at SciVerse ScienceDirect

Talanta

journal homepage: [www.elsevier.com/locate/talanta](http://www.elsevier.com/locate/talanta)

# Quantification of ethanol in petrol–ethanol blends: Use of Reichardt's $E_T(30)$ dye in introducing a petrol batch independent calibration procedure

Keshav Kumar, Ashok Kumar Mishra\*

Department of Chemistry, Indian Institute of Technology-Madras, Chennai, Tamilnadu 600036, India

## ARTICLE INFO

## Article history:

Received 7 July 2012

Received in revised form

6 August 2012

Accepted 7 August 2012

Available online 21 August 2012

## Keywords:

Ethanol

Petrol

Blends

Reichardt's  $E_T(30)$  dye

Polarity

Batch independent quantification

## ABSTRACT

Petroleum fuels are generally non-polar. The presence of ethanol in the petrol–ethanol fuel blends increases the polarity of the fuel blend. It was observed that absorption spectral shift of the Reichardt's  $E_T(30)$  dye is sensitive to the petrol–ethanol blend polarity. It was also found that  $E_T(30)$  dye has a characteristic  $\lambda_{\max}$  of absorption in petrol–ethanol blends irrespective of the petrol batch with which blends were prepared. In the present work, a sensitive analytical method for the petrol batch independent quantification of ethanol content in petrol–ethanol blends has been developed.

© 2012 Elsevier B.V. All rights reserved.

## 1. Introduction

In recent years, ethanol as a renewable fuel has emerged as a potential alternative for hydrocarbon based fuels such as petrol [1–6]. Although ethanol cannot be used as a standalone fuel with the current internal combustion (IC) engine configurations [7,8], ethanol blended petrol is becoming increasingly popular in many countries [1–6]. Depending on the availability of ethanol and other issues such as environmental, social, and technical, ethanol content in blended fuel differs in different parts of the world [9,10]. Ethanol blended petrol as a fuel has better anti-knock properties and it also leads to reduction in the unburned hydrocarbon and carbon monoxide emissions [1,6,10–12]. However, presence of ethanol in petrol causes corrosion of the metallic component of the engine, it also causes swelling and blockage of fuel pipes, and low energy content of ethanol as compared to petrol increases the fuel consumption [1,3,6,13]. Therefore, it is important that ethanol concentration in the blended fuel should not exceed the permissible limit.

Preferential electronic energy state lowering of either ground or excited state of light absorbing molecules by a solvent leads to the phenomena known as solvatochromism [14–22]. The extent of this lowering varies with the polarity of the solvent. 2,6-diphenyl-4-(2,4,6-triphenyl-1-pyridino) phenoxide also known

as Reichardt's  $E_T(30)$  dye is a solvatochromic or polarity probe [15,16].  $E_T(30)$  in its ground state exists as zwitterionic species (shown in Fig. 1A) and upon light absorption it undergoes intramolecular charge transfer (ICT) transition and exists as a biradical species (shown in Fig. 1B) in the excited state [15,21–25]. Consequently,  $E_T(30)$  has larger dipole moment in its ground state than in the excited state [15,21–25]. Polar solvent stabilises the ground state of  $E_T(30)$  to greater extent than the excited state, and therefore as the polarity of the solvents increases it shows blue shift in the light absorption (shown in Fig. 1C) [15,21–25].  $E_T(30)$  is the most sensitive solvatochromic probe which shows more than 350 nm shift while going from nonpolar solvents such as diphenyl ether (810 nm) to water (450 nm) [16]. Because of its high sensitivity, it has been used to study the sol–gel interactions [26] and to measure the polarity of different solvents [16,21,24,27] and solid surfaces [23,28,29]. It has also been used to study the systems such as micelles [25,30–33], polymers [29,34], and dendrimers [35,36] etc.

Petrol is a complex mixture of hydrocarbons and depending on the origin and refining process, the composition of hydrocarbons in different batches of petrol differ [37–39]. Hence analytical techniques developed so far, such as gas chromatography–mass spectrometry (GC–MS) [40], Fourier transform infrared (FTIR) [4,41], near infrared (NIR) [2], and fluorescence [1], have required creating calibration plots specific to a particular batch of petrol. In addition, analyses of FTIR, NIR, fluorescence data sets typically require knowledge of sophisticated chemometric techniques [1,3]. Thus it is important to develop a method which is fast,

\* Corresponding author. Tel.: +91 44 22574207; fax: +91 44 22574202.  
E-mail address: [mishra@iitm.ac.in](mailto:mishra@iitm.ac.in) (A.K. Mishra).

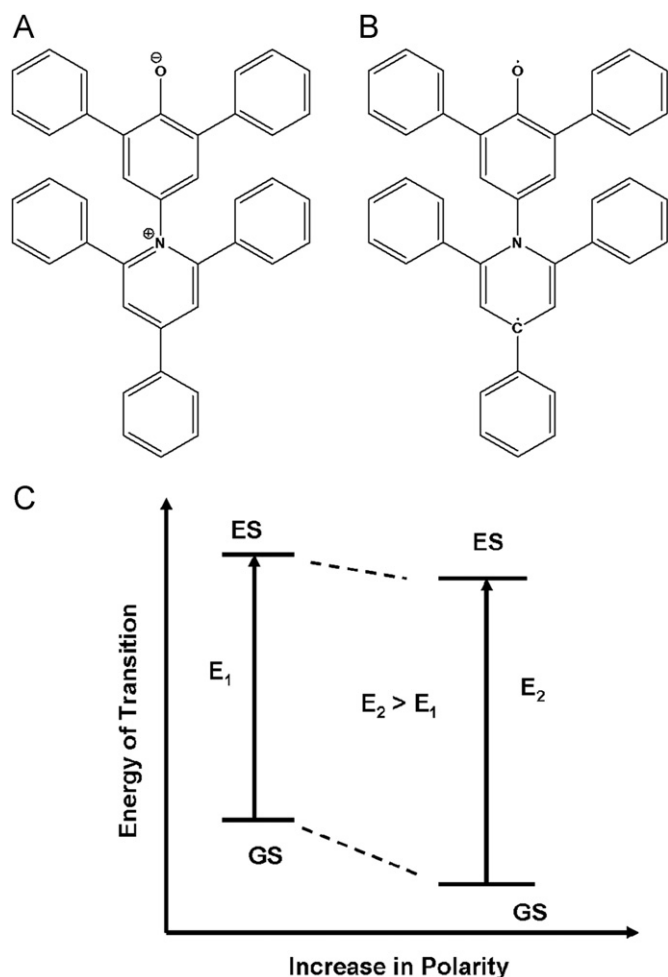


Fig. 1. (A)  $E_T(30)$  in ground state (GS), (B)  $E_T(30)$  in excited state (ES) and (C) variation in energy of transition with increase in polarity.

simple, cost-effective and accurate for the quantification of ethanol in petrol–ethanol blends, irrespective of the batch of the petrol with which blends are made.

Ethanol is more polar than the usual molecular species present in petrol. Hence addition of ethanol would increase the polarity of the fuel. A polarity probe such as  $E_T(30)$  having visible colour change in the range of 450–900 nm should be capable of sensing this change in polarity. Generally petrol is fairly transparent in the visible range of electromagnetic spectrum (530–900 nm) irrespective of the compositional variation of the chromophores from batch to batch. Such an analytical method using a polarity probe would provide a convenient method for quantification of ethanol in petrol, irrespective of the origin of petrol source.

## 2. Experimental

### 2.1. Chemicals and sample preparation

Reichardt's  $E_T(30)$  dye was purchased from the Sigma-Aldrich and ethanol was purchased from the Merck. 10 petrol samples were procured from different local vendors in Chennai and they were labelled as P1, P2, P3, P4, P5, P6, P7, P8, P9 and P10. 13 different petrol–ethanol blends were prepared in the concentration range of 0% to 30% by taking different volumes of ethanol and petrol (P1). Amounts of ethanol and petrol in petrol (P1)–ethanol blends are summarized in Table 1. Blends were labelled

Table 1  
Amount of ethanol in petrol–ethanol blends.

Blend	Petrol (mL)	Ethanol (mL)	Ethanol (v/v) %
E <sub>0</sub>	5.00	0.00	0.00
E <sub>2</sub>	4.90	0.10	2.00
E <sub>4</sub>	4.80	0.20	4.00
E <sub>6</sub>	4.70	0.30	6.00
E <sub>8</sub>	4.60	0.40	8.00
E <sub>10</sub>	4.50	0.50	10.00
E <sub>12</sub>	4.40	0.60	12.00
E <sub>14</sub>	4.30	0.70	14.00
E <sub>16</sub>	4.20	0.80	16.00
E <sub>18</sub>	4.10	0.90	18.00
E <sub>20</sub>	4.00	1.00	20.00
E <sub>25</sub>	3.75	1.25	25.00
E <sub>30</sub>	3.50	1.50	30.00

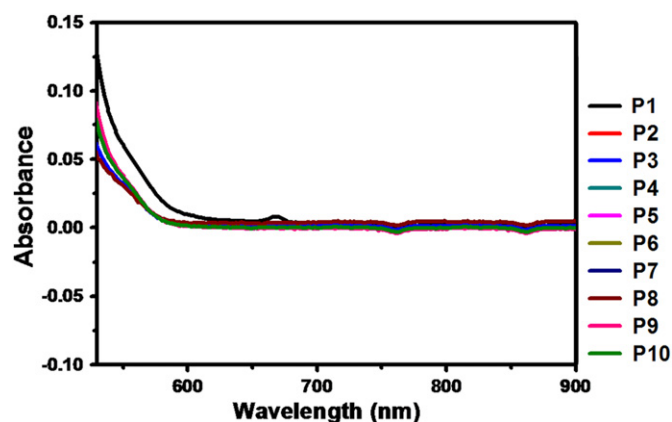


Fig. 2. Absorption spectra of petrol samples.

as E<sub>0</sub>, E<sub>2</sub>, E<sub>4</sub>, E<sub>6</sub>, E<sub>8</sub>, E<sub>10</sub>, E<sub>12</sub>, E<sub>14</sub>, E<sub>16</sub>, E<sub>18</sub>, E<sub>20</sub>, E<sub>25</sub>, and E<sub>30</sub>. Numerical subscript indicates percentage of ethanol in petrol–ethanol blend, for example E<sub>10</sub> contains 10% ethanol in the blended fuel. Similar blends were prepared by taking other petrol samples. In total, 130 blends were prepared.

$E_T(30)$  is insoluble in petrol. Therefore, instead of adding  $E_T(30)$  directly to the petrol and its blends, an aliquot of  $2.8 \times 10^{-3}$  M was made by dissolving 31 mg of  $E_T(30)$  in 20 ml of ethanol. 0.075 ml of the aliquot was added to 5 ml quantity of each of the 130 samples (petrol–ethanol blends).

### 2.2. Instrument and data acquisition

JASCO (V-650) instrument was used for the UV–visible measurements. Absorption spectra were collected in the wavelength range 450–900 nm with a step size of 1 nm using UV cuvette of 1 cm path length. Scan speed was adjusted to 400 nm/min. Before collecting the absorption spectra of  $E_T(30)$  in a given petrol–ethanol blend, baseline correction was done using that particular petrol–ethanol mixture.

## 3. Results and discussion

Fig. 2 shows the absorption spectra of P1–P10 petrol samples. It can be seen that all the ten petrol samples are fairly transparent in the wavelength range of 530–900 nm. Fig. 3 contains the absorption spectra of  $E_T(30)$  in all the 13 petrol–ethanol blends made using petrol P1. A blue shift in the absorbance  $\lambda_{\max}$  for  $E_T(30)$  is observed with increasing ethanol concentration in the petrol–ethanol mixtures. As shown in Fig. 1C, blue shift arises

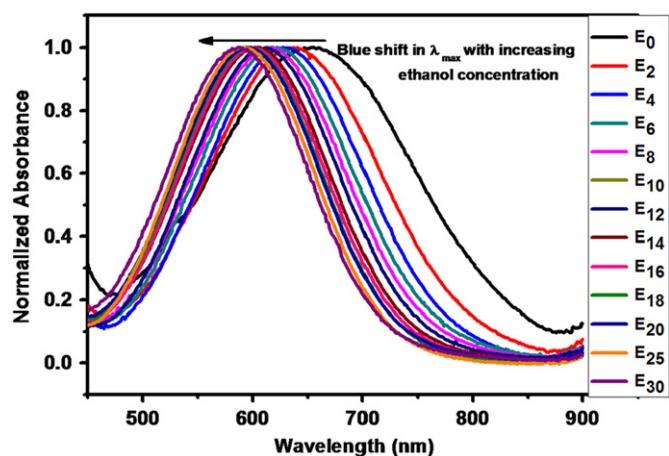


Fig. 3. Normalized absorption spectra of  $E_T(30)$  in various blends of P1 (petrol).

Table 2

$\lambda_{\max}$  (nm) of absorption of  $E_T(30)$  in various blends of 10 different petrol samples.

Blend	P1	P2	P3	P4	P5	P6	P7	P8	P9	P10
$E_0$	655	663	662	646	667	658	657	659	656	665
$E_2$	631	634	635	634	636	638	638	637	637	638
$E_4$	628	629	629	629	629	630	630	629	631	634
$E_6$	621	620	619	620	621	622	622	622	622	624
$E_8$	614	615	616	616	615	619	617	618	618	617
$E_{10}$	612	613	611	612	610	611	616	613	615	613
$E_{12}$	606	607	609	608	608	609	607	608	607	613
$E_{14}$	604	605	606	605	604	605	605	607	604	606
$E_{16}$	600	601	601	601	601	602	601	602	603	601
$E_{18}$	596	597	598	598	599	600	599	600	601	600
$E_{20}$	594	594	596	596	596	597	597	594	596	599
$E_{25}$	591	591	591	591	593	593	591	593	593	594
$E_{30}$	588	588	588	588	588	589	587	588	588	589

because of the increase in energy difference between the ground state and excited state of  $E_T(30)$  with the increase in polarity of petrol–ethanol blends. Similar blue shift in the absorbance  $\lambda_{\max}$  for  $E_T(30)$  with the ethanol concentration were observed in the various blends prepared using P2–P10 petrol. Absorption spectra of  $E_T(30)$  in these blends are given in Fig. S11. Absorbance  $\lambda_{\max}$  of  $E_T(30)$  in all the 130 samples are summarized in Table 2. From the table it can be seen that  $E_T(30)$  has a characteristic  $\lambda_{\max}$  in all the blends irrespective of the petrol sample with which these blends were made. The absorbance  $\lambda_{\max}$  of  $E_T(30)$  in the unblended  $E_0$  samples show much lower energy transitions ( $\sim 646$ – $667$  nm range) as compared to even the 2% ethanol blend ( $\sim 631$ – $638$  nm range) (Table 2). The small variation of  $E_0$  from batch to batch is probably due to the compositional variation of polar molecules in different batches.

Absorbance  $\lambda_{\max}$  of  $E_T(30)$  in various blends of petrol P1 were converted into energy of transition ( $E_T$ ) in Kcal/mol units using Eq. (1) [16].

$$E_T = \frac{28,591}{\lambda_{\max}} \quad (1)$$

$E_T$  values of  $E_T(30)$  in various blends of petrol P1 were plotted against the concentration of ethanol and are shown in Fig. 4. The plot shows a fairly regular though nonlinear variation of the transition energy ( $E_T$ ) with ethanol concentration. This nonlinearity is known to be due to the preferential solvation of  $E_T(30)$  by more polar ethanol molecules [14,19,24,42,43]. Preferential solvation by ethanol molecules arises due to the presence of negatively charged phenoxide moiety in  $E_T(30)$  which forms

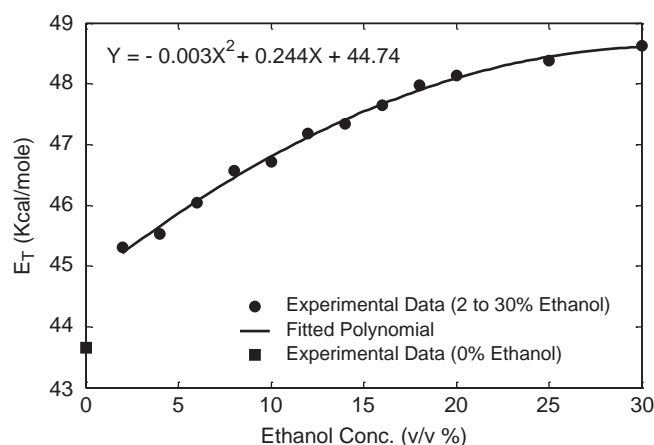


Fig. 4. Variation of  $E_T$  of  $E_T(30)$  with ethanol concentration in petrol–ethanol blends.

hydrogen bond with ethanol molecules [14,19,24,42,43].  $E_T$  values for  $E_T(30)$  in all the blends of other petrol samples were also calculated and are summarized in Table 3. Due to the variation in the absorbance  $\lambda_{\max}$  of  $E_T(30)$  in  $E_0$  samples of different batches,  $E_T$  value of  $E_T(30)$  in  $E_0$  sample of P1 was not included, and we tried to make the calibration model for the quantification of ethanol in the concentration range of 2% to 30%. Moreover, blends which are commonly used are  $E_5$ ,  $E_{10}$ ,  $E_{15}$ , and  $E_{20}$  therefore quantification of ethanol in the concentration range of less than 2% is not much of practical importance.

$E_T$  values of  $E_T(30)$  in the blends of P1 were fitted against the ethanol concentrations with the polynomials of various orders. To find the order of the polynomial which gives the best fit, statistical parameter  $R^2$  (square of the correlation coefficient) [44] was plotted against the order of the fitted polynomials, shown in Fig. 5. From the figure it can be seen that (i) polynomial of first order fits the data with minimum  $R^2$  (0.9230), (ii) polynomial of second order fits the data with maximum  $R^2$  value of 0.9937, and (iii) after second order  $R^2$  value decreases with the increase in the order of the polynomials. Therefore, second order polynomial given in Eq. (2) which provides maximum  $R^2$ , was used to explain the variation of  $E_T$  with ethanol concentration (shown in Fig. 4),

$$Y = -0.003X^2 + 0.244X + 44.74 \quad (2)$$

where  $Y$  is the  $E_T$  value and  $X$  is the ethanol concentration.

Using Eq. (2) and  $E_T$  values from Table 3, predicted ethanol concentrations in all the 12 blends of petrol P1 were calculated. It should be noted that second order polynomial (Eq. (2)) has two roots (ethanol concentration) and one of the roots would be unacceptable which can easily be discarded using the information of absorbance  $\lambda_{\max}$  of  $E_T(30)$  in petrol–ethanol mixtures. Actual and predicted (calculated) concentrations of ethanol were plotted and are given in Fig. 6. Root mean square error of calibration (RMSEC) [45], a measure of accuracy with which a calibration model predicts the concentration of a component in calibration set samples, was calculated using the Eq. (3).

$$\text{RMSEC or RMSEP} = \sqrt{\frac{\sum_{i=1}^n (X_{\text{actual}} - X_{\text{predicted}})^2}{n}} \quad (3)$$

where  $n$  is the number of samples, in the present case  $n$  is 12,  $X_{\text{actual}}$  and  $X_{\text{predicted}}$  are the actual and predicted ethanol concentration in the blends of P1. RMSEC value was found to be 0.79 which shows that calibration model predicted the ethanol concentration of the calibration set samples accurately.

**Table 3**  
Transition energy (Kcal/mole) of  $E_T(30)$  in various blends of 10 different petrol samples.

Blend	P1	P2	P3	P4	P5	P6	P7	P8	P9	P10
E0	43.65	43.12	43.19	44.26	42.87	43.45	43.52	43.39	43.58	42.99
E <sub>2</sub>	45.31	45.10	45.03	45.10	44.95	44.81	44.81	44.88	44.88	44.81
E <sub>4</sub>	45.53	45.45	45.45	45.45	45.45	45.38	45.38	45.45	45.31	45.10
E <sub>6</sub>	46.04	46.11	46.19	46.11	46.04	45.97	45.97	45.97	45.97	45.82
E <sub>8</sub>	46.57	46.49	46.41	46.41	46.49	46.19	46.34	46.26	46.26	46.34
E <sub>10</sub>	46.72	46.64	46.79	46.72	46.87	46.79	46.41	46.64	46.49	46.64
E <sub>12</sub>	47.18	47.10	46.95	47.02	47.02	46.95	47.10	47.02	47.10	46.64
E <sub>14</sub>	47.34	47.26	47.18	47.26	47.34	47.26	47.26	47.10	47.34	47.18
E <sub>16</sub>	47.65	47.57	47.57	47.57	47.57	47.49	47.57	47.49	47.41	47.57
E <sub>18</sub>	47.97	47.89	47.81	47.81	47.73	47.65	47.73	47.65	47.57	47.65
E <sub>20</sub>	48.13	48.13	47.97	47.97	47.97	47.89	47.89	48.13	47.97	47.73
E <sub>25</sub>	48.38	48.38	48.38	48.38	48.21	48.21	48.38	48.21	48.21	48.13
E <sub>30</sub>	48.62	48.62	48.62	48.62	48.62	48.54	48.71	48.62	48.62	48.54

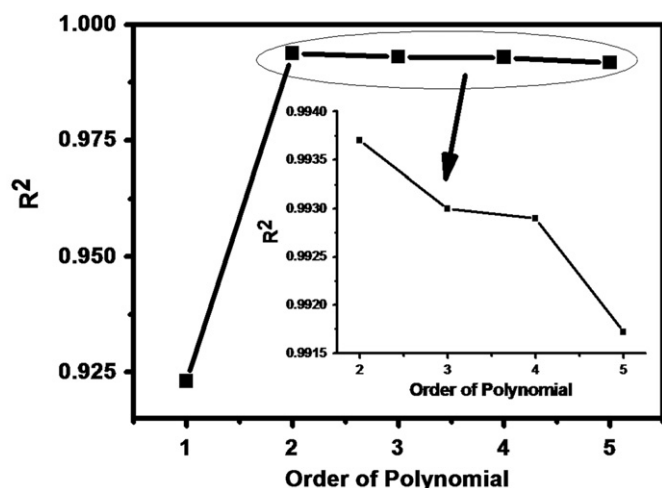


Fig. 5. Variation of  $R^2$  with the order of the fitted polynomial.

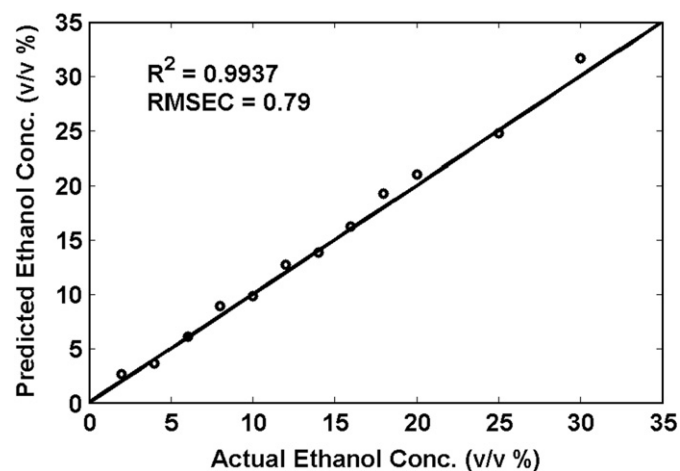


Fig. 6. Actual and predicted concentration of ethanol in petrol-ethanol blends.

In order to test the prediction ability of calibration model based on P1 blends, 9 different validations set each consisting of 12 samples were used. Using Eq. 2 and  $E_T$  values of the blends from Table 3, concentration of ethanol in all the 108 samples (12 blends of each of the 9 petrol samples) were calculated and are reported in Table 4. The root mean square error of prediction (RMSEP) value [45], a measure of the accuracy with which calibration model predicts the concentration of the unknown samples was calculated for each batch of the petrol by using

Eq. 3. For P2–P10 petrol based blends RMSEP values were found to be 0.73, 0.80, 0.66, 1.14, 1.36, 1.11, 1.40, 1.50, and 2.02, respectively. Overall RMSEP was found to be less than 2.0%. Small RMSEP values show that irrespective of the petrol with which blends were made, obtained calibration model is capable of estimating ethanol concentration in unknown petrol-ethanol blends with small error in estimation.

In this work, petrol batch (source) independent quantifications of ethanol in blended petrol were achieved for the concentration range of 2% to 30%. Typical blends which are used in vehicles E<sub>5</sub>, E<sub>10</sub>, E<sub>15</sub>, and E<sub>20</sub> therefore the obtained calibration model is well capable of ensuring the fuel quality. Moreover, Table 2 which contains the  $\lambda_{\max}$  of  $E_T(30)$  in various blends can be used even by a layman for the estimation of ethanol content in ethanol blended petrol. From the table it can be seen that  $E_T(30)$  has  $\lambda_{\max}$  in the range of 586–643 nm for 2% to 30% ethanol blended petrol. Absorbance  $\lambda_{\max}$  of  $E_T(30)$  appears above 650 nm in the petrol blends which contains less than 2% of ethanol.  $E_T(30)$  in 10% and 20% petrol-ethanol blends, show absorbance  $\lambda_{\max}$  around 612 and 596 nm, respectively. On the other hand,  $\lambda_{\max}$  will appear below 580 nm, if petrol is blended with more than 30% ethanol. It is also important to mention that there may be some variation in the  $\lambda_{\max}$  of absorption for  $E_T(30)$  in a particular petrol-ethanol mixture if the concentration of  $E_T(30)$  aliquot is changed. Thus, in order to avoid any ambiguity it is necessary that 0.075 ml of  $2.8 \times 10^{-3}$  M ethanolic  $E_T(30)$  solution should be added to the 5 ml of petrol-ethanol mixture. However, a calibration model can always be made with any other appropriate concentration of  $E_T(30)$  dye solution. It will also be interesting to see whether the solvent polarity probes can be used for the diesel batch independent ethanol quantification in diesel-ethanol blends where solubilizers are added to overcome the solubility problem between ethanol and diesel.

#### 4. Conclusions

Petrol is a complex mixture of hydrocarbons and composition of which changes from batch to batch; however, it was found that Reichardt's  $E_T(30)$  dye has a characteristic  $\lambda_{\max}$  of absorption in each petrol-ethanol blend irrespective of the petrol sample used to create that blend. With the increase in the ethanol concentration in petrol-ethanol blends  $E_T(30)$  shows a blue shift in the absorbance  $\lambda_{\max}$ . A calibration model was developed for the petrol batch independent ethanol quantification in petrol-ethanol blends by studying the variation of transition energy of  $E_T(30)$  dye as a function of ethanol concentration. Statistical parameters such as  $R^2$ , RMSEC, and RMSEP indicate that the calibration model developed is fairly robust.

**Table 4**

Actual and predicted ethanol concentration in 108 blends of validation set.

Blend	Actual ethanol conc. (v/v %)	Predicted ethanol conc.(v/v%)								
		P2	P3	P4	P5	P6	P7	P8	P9	P10
E <sub>2</sub>	2.00	1.68	1.38	1.68	1.04	0.45	0.45	0.75	0.75	-0.92
E <sub>4</sub>	4.00	3.24	3.24	3.24	3.24	2.92	2.92	3.24	2.61	2.92
E <sub>6</sub>	6.00	6.43	6.85	6.43	6.07	5.72	5.72	5.72	5.72	4.98
E <sub>8</sub>	8.00	8.47	8.02	8.02	8.45	6.85	7.64	7.21	7.21	7.64
E <sub>10</sub>	10.00	9.32	10.21	9.79	10.70	10.21	8.02	9.32	8.47	9.32
E <sub>12</sub>	12.00	12.17	11.2	11.65	11.65	11.20	12.17	11.65	12.17	9.32
E <sub>14</sub>	14.00	13.27	12.71	13.27	13.84	13.27	13.27	12.17	13.84	12.71
E <sub>16</sub>	16.00	15.60	15.60	15.60	15.60	14.97	15.6	14.97	14.36	15.60
E <sub>18</sub>	18.00	18.44	17.67	17.67	16.95	16.26	16.95	16.26	15.60	16.26
E <sub>20</sub>	20.00	21.05	19.25	19.25	19.25	18.44	18.44	21.05	19.24	16.95
E <sub>25</sub>	25.00	24.74	24.74	24.74	22.07	22.07	24.74	22.07	22.07	21.04
E <sub>30</sub>	30.00	31.69	31.69	31.69	31.69	29.09	31.69	31.69	31.69	29.09

## Acknowledgements

Keshav Kumar is thankful to the Council of Scientific and Industrial Research (CSIR) New Delhi for providing the fellowship. The authors thank CSIR for the financial support to carry out the work.

## Appendix A. Supporting information

Supplementary data associated with this article can be found in the online version at <http://dx.doi.org/10.1016/j.talanta.2012.08.007>.

## References

- [1] K. Kumar, A.K. Mishra, J. Fluoresc. 22 (2012) 339–347.
- [2] H.L. Fernandes, I.M. Raimundo Jr., C. Pasquini, J.J.R. Rohwedder, Talanta 75 (2008) 804–810.
- [3] P.F. Pereira, M.C. Marra, R.A.A. Munoz, E.M. Richter, Talanta 90 (2012) 99–102.
- [4] P.R. Prasad, K.S.R. Rao, K. Bhuvaneshwari, N. Praveena, Y.V.V. Srikanth, Energy Sources A 30 (2008) 1534–1539.
- [5] H.G. Aleme, L.M. Costa, P.J.S. Barbeira, Talanta 78 (2009) 1422–1428.
- [6] F. Yüskel, B. Yüskel, Renew. Energy 29 (2004) 1181–1191.
- [7] R. French, P. Malone, Fluid Phase Equilib. 228–229 (2005) 27–40.
- [8] S. Kumar, N. Singh, R. Prasad, Renew. Sustain. Energy Rev. 14 (2010) 1830–1844.
- [9] S. Pohit, P.K. Biswas, R. Kumar, J. Jha, Energy Policy 37 (2009) 4540–4548.
- [10] M. Al-Hasan, Energy Convers. Manage. 44 (2003) 1547–1561.
- [11] S. Gouli, E. Lois, S. Stourmas, Energy Fuels 12 (1998) 918–924.
- [12] D.C. Drown, K. Harper, E. Frame, J. Am. Oil Chem. Soc. 78 (2001) 579–584.
- [13] T.R.L.C. Paixao, J.L. Cardoso, M. Bertotti, Fuel 86 (2007) 1181–1185.
- [14] O.A. El Seoud, Pure Appl. Chem. 81 (2009) 697–707.
- [15] S. Nigam, S. Rutan, Appl. Spectrosc. 55 (2001) 362A–370A.
- [16] C. Reichardt, Chem. Rev. 94 (1994) 2319–2358.
- [17] P. Suppan, J. Photochem. Photobiol. A Chem. 50 (1990) 293–330.
- [18] H.M. Reza, C.M. Javed, Y. Maryam, Iran. J. Chem. Chem. Eng. 27 (2008) 9–14.
- [19] C. Reichardt, Green Chem. 7 (2005) 339–351.
- [20] C. Reichardt, Pure Appl. Chem. 80 (2008) 1415–1432.
- [21] M.F. Vitha, J. Chem. Educ. 78 (2001) 370–372.
- [22] C. Reichardt, Solvents, Solvent Effects in Organic Chemistry, 2nd ed., VCH, New York, 1988.
- [23] D.J. Macquarrie, S.J. Tavener, G.W. Gray, P.A. Heath, J.S. Rafelt, S.I. Saulzet, J.J.E. Hardy, J.H. Clark, P. Sutra, D. Brunel, F. di Renzo, F. Faiula, New J. Chem. 23 (1999) 725–731.
- [24] C. Reichardt, Pure Appl. Chem. 65 (1993) 2593–2601.
- [25] L. Luchetti, Colloid Surf. A 297 (2007) 249–252.
- [26] C. Rottman, G.S. Grader, Y.D. Hazan, D. Avnir, Langmuir 12 (1996) 5505–5508.
- [27] E.B. Tada, L.P. Novaki, O.A. El Seoud, J. Phys. Org. Chem. 13 (2000) 679–687.
- [28] S.J. Tavener, J.H. Clark, G.W. Gray, P.A. Heath, D.J. Macquarrie, Chem. Commun. 12 (1997) 1147–1148.
- [29] S. Nishiyama, S. Aikawa, Y. Yoshida, M. Tajima, Mol. Cryst. Liq. Cryst. 462 (2007) 257–265.
- [30] L.P. Novaki, O.A. El Seoud, Phys. Chem. Chem. Phys. 1 (1999) 1957–1964.
- [31] L.P. Novaki, O.A. El Seoud, Langmuir 16 (2000) 35–41.
- [32] E.B. Tada, L.P. Novaki, O.A. El Seoud, Langmuir 17 (2001) 652–658.
- [33] J.K. Basu, M. Shannigrahi, N. Ray, S. Bagchi, Spectrochim. Acta A 61 (2005) 2539–2542.
- [34] B. Szczupak, A.G. Ryder, D.M. Togashi, Y.A. Rochev, A.V. Gorelov, T.J. Glynn, Appl. Spectrosc. 63 (2009) 442–449.
- [35] D.L. Richter-Egger, H. Li, S.A. Tucker, Appl. Spectrosc. 8 (2000) 1151–1156.
- [36] C. Reichardt, E.H. Gerner, Leibigs Ann. Chem. 5 (1983) 721–743.
- [37] W.R. Hartley, A.J. Englande, Water Sci. Technol. 25 (1992) 65–72.
- [38] R.M. Alberici, C.G. Zampronio, R.J. Poppi, M.N. Eberlin, Analyst 127 (2002) 230–234.
- [39] O. Divya, A.K. Mishra, Anal. Chim. Acta 592 (2007) 82–90.
- [40] V.L. Skrobot, E.V.R. Castro, R.C.C. Pereira, V.M.D. Pasa, I.C.P. Fortes, Energy Fuels 19 (2005) 2350–2356.
- [41] J.W. Diehl, J.W. Finkbeiner, F.P. Disanzo, Anal. Chem. 64 (1992) 3202–3205.
- [42] P.D. Galgano, C. Loffredo, B.M. Sato, C. Reichardt, O.A. El Seoud, Chem. Educ. Res. Pract. 13 (2012) 147–153.
- [43] R. Budag, L.A. Giusti, V.G. Machado, C. Machado, Fuel 85 (2006) 1494–1497.
- [44] R.G.D. Steel, J.H. Torrie, Principles, Procedures of Statistics, McGraw-Hill, New York, 1960.
- [45] R. Kramer, Chemometric Techniques for Quantitative Analysis, Marcel Decker Inc., New York, 1998.